Long-period astronomical forcing of mammal turnover

Jan A. van Dam[1], Hayfaa Abdul Aziz[1]†, M. Ángeles Álvarez Sierra[2], Frederik J. Hilgen[1], Lars W. van den Hoek Ostende[3], Lucas J. Lourens[1], Pierre Mein[4], Albert J. van der Meulen[1] & Pablo Pelaez-Campomanes[5]

Mammals are among the fastest-radiating groups, being characterized by a mean species lifespan of the order of 2.5 million years (Myr)[1,2]. The basis for this characteristic timescale of origination, extinction and turnover is not well understood. Various studies have invoked climate change to explain mammalian species turnover[3,4], but other studies have either challenged or only partly confirmed the climate–turnover hypothesis[5–7]. Here we use an exceptionally long (24.5–2.5 Myr ago), dense, and well-dated terrestrial record of rodent lineages from central Spain, and show the existence of turnover cycles with periods of 2.4–2.5 and 1.0 Myr. We link these cycles to low-frequency modulations of Milankovitch oscillations[8], and show that pulses of turnover occur at minima of the 2.37-Myr eccentricity cycle and nodes of the 1.2-Myr obliquity cycle. Because obliquity nodes and eccentricity minima are associated with ice sheet expansion and cooling and affect regional precipitation, we infer that long-period astronomical climate forcing is a major determinant of species turnover in small mammals and probably other groups as well.

Changes in organisms occur on a variety of temporal scales. Four basic temporal scales (tiers) have been recognized: the ecological timescale; the Milankovitch timescale of precession (the wobbling of the Earth's axis, ~21 kyr periodicity), obliquity (tilt of the Earth's axis, 41 kyr periodicity) and eccentricity (the orbit around the Sun, ~100 and ~400 kyr periodicity); the million-year timescale of species extinctions and originations; and the ultra-long timescale of mass extinctions and major taxonomic replacements[9]. Although the main processes controlling the first tier (climate change and competition), the second tier (climate-forced distributional variation)[3,9,10] and the fourth tier (catastrophic perturbations of the Earth's biosphere) are reasonably well defined, the mechanisms underlying third-tier processes are not well understood. Mammals have featured importantly in discussions on the processes pertaining to this tier[2–7]. Because their mean species duration is estimated at 2.3–2.6 Myr (refs 1, 2), primary (20–400kyr) Milankovitch variations cannot be held responsible for mammal speciation and extinction[4,9,10]. It has been suggested that amplitude changes of climatic oscillations could have played a part in explaining turnover[3,10], but until now no efforts have been made systematically to compare such amplitude variations with turnover in long and well-dated records.

We compiled a data set of more than 200 rodent assemblages from Central Spain (see Supplementary Notes and Supplementary Table 1) and analysed it in terms of turnover. The record is exceptionally long (22 Myr), largely continuous, dense and well dated. We focused on rodents, because screen sieving allows the collection of large amounts of easily identifiable dental elements. The studied fossils originate from fluvio-lacustrine sections in the Madrid, Calatayud-Daroca and Teruel basins, and amount to over 80,000 isolated molars, which were identified at the species and lineage level (132 lineages, pseudo-extinctions ignored). All studied localities are positioned in stratigraphic sections, a large number of which have been tied to the geomagnetic polarity timescale by first-order correlations. The complete temporal sequence was calibrated to the new astronomically tuned timescale for the Neogene[11] (Supplementary Fig. 1). The use of this new timescale is of crucial importance because it allows a direct comparison with time series of the Earth's orbital parameters outlined above.

Randomization procedures were used to capture uncertainties in the ages of localities (by the generation of a series of equally probable age models) and of first and last rodent appearances, resulting in 1,000 equally probable time series. Sample size effects on the presence or absence of rodents were observed to be fairly small and were further reduced by inferring lineage presence on a range-through basis and by excluding the rarest occurrences (see Methods, Supplementary Notes and Supplementary Figs 4 and 5). We chose 0.1 Myr as our basic time unit and calculated a mean time series of standing diversity, and mean time series of total and per-taxon rates of origination, extinction and their aggregate (turnover; Figs 1 and 3b; Supplementary Figs 2 and 3). Re-entry by migration was assumed for lineages with an estimated absence of more than 1.0 Myr, resulting in 22 to 33 additional lineage segments, depending on the age model (see Methods and Supplementary Notes for details on age uncertainties and turnover calculations). It is not possible to make an accurate estimation of either the relative contributions of migration and speciation to the origination record or of local and true extinction to the extinction record, because of problems of poor dating and low resolution of time-equivalent records outside the study area. However, at the scale of Mammal Neogene (MN) European zones (mean duration of 1.3 Myr) we estimated that ~20% of both the entries and exits in the study region represent immigration or local extinction, respectively (excluding migration by re-entry). Almost 40% of the lineages are endemic to Spain. Their first- and last-occurrence ages and those of the remaining 40% can be considered to lie relatively close to the ages of speciation and true extinction.

The origination, extinction and turnover time series are characterized by distinct peaks spaced by ~1–2 Myr (Figs 1 and 3b;

Supplementary Figs 2 and 3). The rounded shape of the Early Miocene epoch turnover maxima can be attributed to the relatively large age uncertainties in this interval. Mostly, but not always, origination and extinction peaks coincide or have almost the same age. Using a bootstrap approach (see Methods and Supplementary Notes), we found that 11 entry, exit or turnover peaks were significant at the 99% level. At the 95%, 90% and 80% level, the total number of such significant events was 21, 29 and 33, respectively (Supplementary Table 2). We performed spectral analysis on the turnover rate series to test for million-year scale periodicities and found significant frequencies corresponding to periods of 2.4 or 2.5 Myr and 1.0 Myr (Fig. 2a, b). The individual extinction and origination spectra show a similar distribution of power (Supplementary Fig. 6). Most turnover maxima are associated with an increase in the proportion of short-lived species as indicated by the simultaneous occurrence of peaks in diversity and troughs in mean lifespan per 0.1 Myr (Fig. 1). The overall mean residence time is 2.0 Myr.

From astronomical calculations it is known that the amplitudes of the ~100 and 405 kyr eccentricity cycles occur superposed on long-period cycles with periods of 2.37 and 0.97 Myr (ref. 8; Figs 2a and 3e). In combination, these longer cycles produce prolonged intervals of low eccentricity that are either ~2.0 or ~2.8 Myr apart (Fig. 3e, blue stripes). The almost identical periods observed in the spectra of eccentricity and rodent turnover (Fig. 2a), as well as the recent documentation of the expression of the 2.37-Myr eccentricity cycle in continental and marine lithological sequences, and marine microfossil abundances[12–14], suggests that long-period eccentricity modulation had a significant influence on the rodent record. This notion is confirmed by cross-spectral analysis of the eccentricity envelope and per-taxon turnover series, which produces maximum and significant coherences at periods of 2.38 and 0.97 Myr, respectively (Fig. 2c). The phase spectrum, however, reveals that turnover is in anti-phase with the 2.37-Myr eccentricity cycle (0.05 ± 0.12 Myr, 2σ) and in phase (0.06 ± 0.03 Myr) with the 0.97-Myr cycle (Figs 2c and 3c, e), excluding the possibility of a common forcing mechanism. On the other hand, eccentricity maxima occurring every 0.97-Myr that correlate to significant turnover events at 15.9–15.8, 14.8–14.7, 13.8–13.7, 9.0–8.7, 7.8–7.7, 4.3–4.1 and 3.3–3.1 Myr ago also coincide with distinct nodes (points of minimum variation) of the 1.2-Myr modulation cycle of obliquity[8] (Fig. 3c, e, f; green stripes). The obliquity nodes are spaced 1.0 or 1.4 Myr apart in alternating fashion owing to a 2.4-Myr period (Figs 2b and 3f) produced by resonance with the equally long eccentricity cycle[8]. The appearance of the 0.98-Myr period in the turnover spectra can therefore also be explained by the 1.0-Myr spacing between obliquity nodes. Pairs of 1.0-Myr spaced combinations of eccentricity maxima and obliquity nodes occur once every 4 Myr on average at 20.6 and 19.6, 16.0 and 15.1, 13.7 and 12.7, 9.0 and 7.9, and 4.2 and 3.2 Myr ago (Fig. 3e, f). The cross spectrum of obliquity and turnover is consistent with obliquity influence, showing maximum and significant coherence at a frequency corresponding to a period of 1.17 Myr without any phase difference (0.01 ± 0.06 Myr; Fig. 2d). A faunal response to the 1.2-Myr obliquity cycle is to be expected because this cycle, in

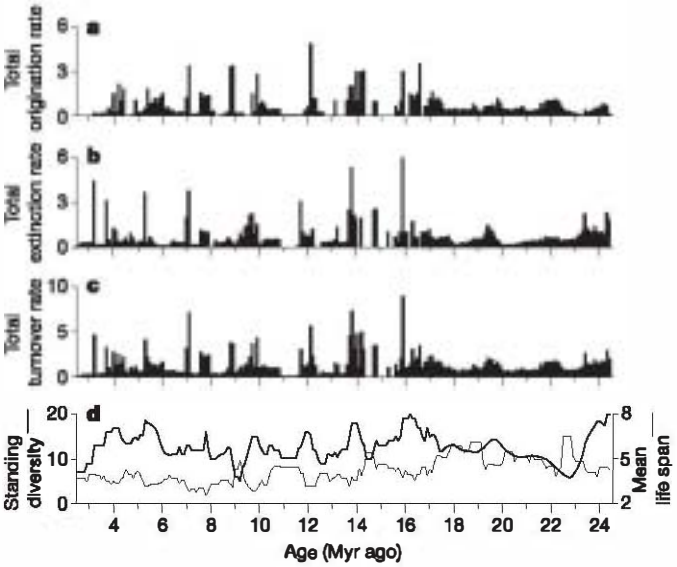

Figure 1 | Lineage turnover, diversity and mean lifespan per 0.1 Myr. The mean number of events and mean standing diversity are inferred from 1,000 equally probable series. The mean lifespan is based on an age model resulting in an average number of re-entering lineages, and calculated as the average lifespan of all lineages present. Origination ages before 24.4 Myr ago are based on the Oligocene rodent record from Central Spain and extinction ages after 2.5 Myr ago are based on the Pliocene–Pleistocene record of Southern Spain. **a**, Number of originations per 0.1 Myr. **b**, Number of extinctions per 0.1 Myr. **c**, Number of originations plus number of extinctions (turnover) per 0.1 Myr. **d**, Standing diversity (number of lineages) and mean lifespan (Myr).

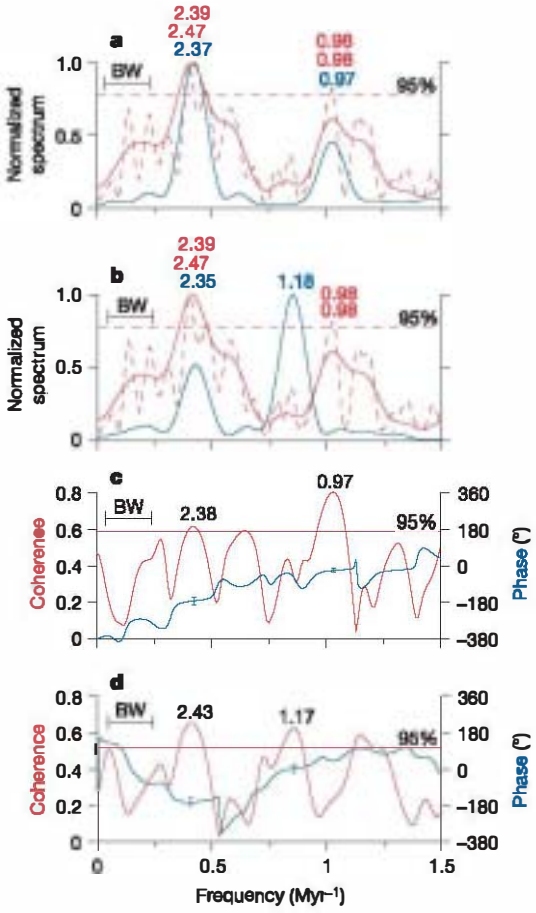

Figure 2 | Individual and cross spectra of turnover, eccentricity and obliquity. Methods used were Blackman–Tukey (solid lines), and CLEAN[39] (dashed lines). Numbers refer to significant periods (Myr). BW, bandwidth (for Blackman-Tukey). **a**, Red lines, per-taxon turnover. Blue line, eccentricity envelope (~100 kyr maxima). **b**, Red lines as in **a**. Blue line, obliquity envelope (41 kyr minima). **c**, Red line, coherence between per-taxon turnover and eccentricity maxima with 95% significance level for non-zero coherence. Blue line, phase difference; error bars (95% confidence level) are indicated for the relevant frequencies. **d**, Red line, coherence between per-taxon turnover and obliquity minima with 95% significance level for non-zero coherence. Blue line, phase difference; error bars (95% confidence level) are indicated for the relevant frequencies.

contrast to the 0.97-Myr eccentricity cycle, is well documented in marine sedimentary sequences[12,14–18].

How can reduced orbital variation at obliquity nodes and long-term eccentricity minima trigger biological turnover? The geological record suggests an important role for climatic change. Owing to the construction of high-resolution, astronomically tuned deep-sea records, many Cenozoic events of increasing $\delta^{18}O$ values (Oligocene isotope, Miocene isotope and related events) have been correlated to obliquity nodes with a mean spacing of 1.2 Myr[14–18] (Fig. 3f, g; Supplementary Table 2). These million-year-scale events represent short (at most one to two hundred thousand years) episodes of ice-sheet expansion and cooling superposed on the main Cenozoic-era cooling trend[19] (Fig. 3h). The occurrence of these events is also related to eccentricity, because most of them seem to coincide with minima of the 405-kyr eccentricity cycle[15–18]. The development of ice sheets can be explained by assuming a sustained reduction of ice melting during relatively cool high-latitude summers[14,15]. It seems that almost all glacial events that are linked to the strongest combinations of an obliquity node and a 405-kyr eccentricity minimum (Fig. 3d) are associated with statistically significant turnover events in the well-dated part (after 17 Myr ago) of the rodent record (Supplementary Table 2).

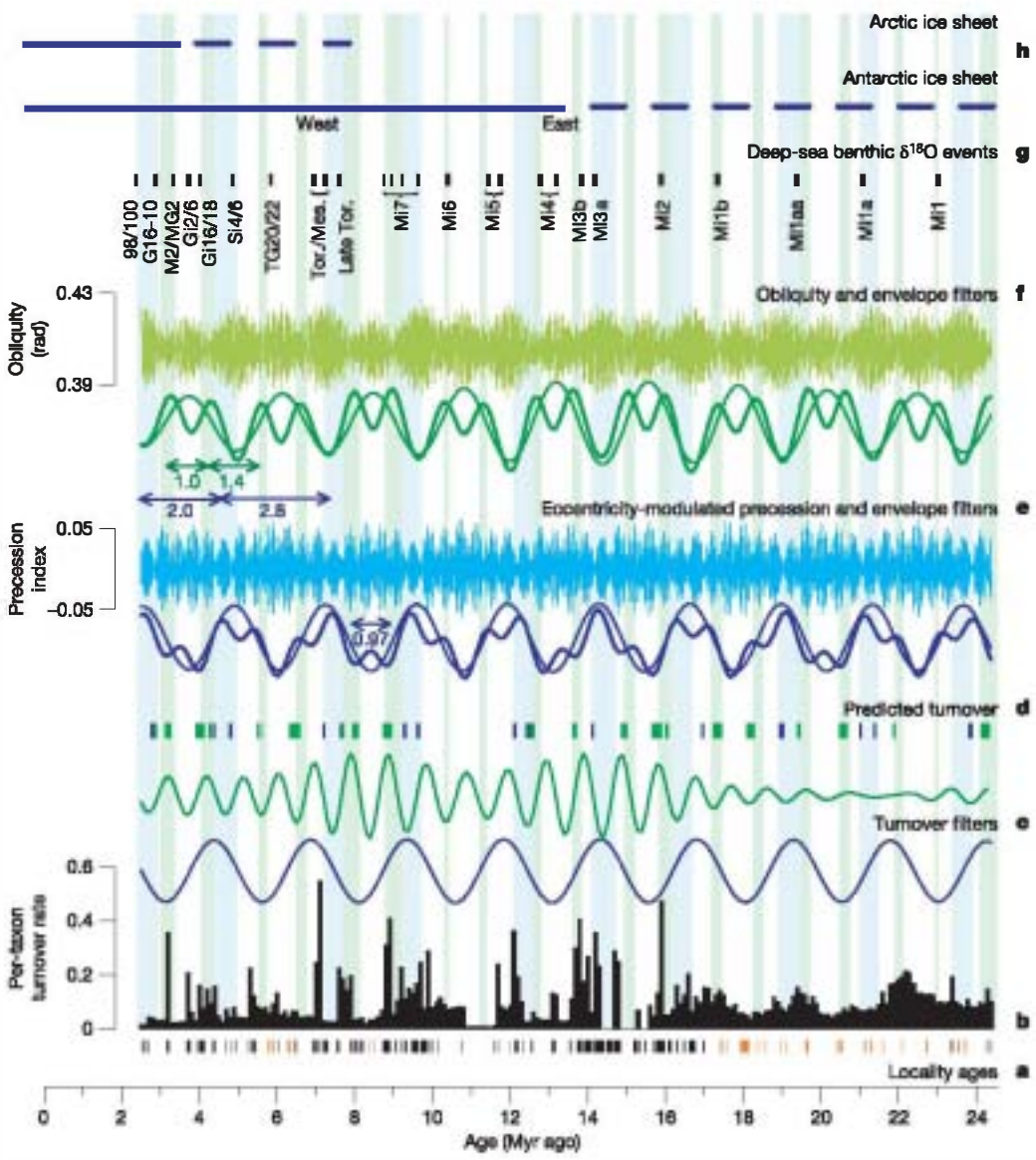

Figure 3 | Rodent turnover, astronomical parameters and climate. Blue stripes, eccentricity minima (mean spacing of 2.37 Myr), Green stripes, obliquity nodes (mean spacing of 1.2 Myr). **a**, Estimated ages of rodent localities. Black bars, from a single preferred correlation; orange bars, means after randomization (see Supplementary Notes and Supplementary Table 1). **b**, Per-taxon turnover rate (per 0.1 Myr). **c**, Filtered per-taxon turnover record. Blue, 99% significance filter, CLEAN method[30]; green, filtered 0.97-Myr component, centred at 1.03 ± 0.15 Myr $^{-1}$. **d**, Predicted times of turnover. Blue bars, mean eccentricity <0.12 during preceding 100 kyr; green bars, mean 41-kyr obliquity minimum >0.396 rad during preceding 400 kyr combined with mean eccentricity <0.30 during preceding 100 kyr. **e**, Eccentricity-modulated precession and filters, CLEAN method[30]. Upper curve, eccentricity-modulated precession[5]; lower thin blue line, 99% significance filter of eccentricity maxima (reversed); lower thick blue line, 95% significance filter of eccentricity maxima (reversed). **f**, Obliquity and filters. Upper curve, obliquity[5]; lower thick green line, 90% significance filter of obliquity minima; lower thin green line, filtered 2.4-Myr component, centred at 0.43 ± 0.1 Myr $^{-1}$. **g**, Major deep-sea $\delta^{18}O$ events. Mi, Miocene isotope; Tor., Tortonian; Mes., Messinian; TG, Thvera-Gauss; Si, Sidufjall; Gi, Gilbert; M, Mammoth; MG, Mammoth-Gauss; G, Gauss. **h**, Ice-sheet history[19]. Upper blue line, Arctic ice sheet; lower blue line, Antarctic ice sheet; continuous line, full-scale or permanent ice; dashed line, partial or ephemeral ice.

Positive feedback effects on the global climate of ice sheet expansion during obliquity nodes are expected to lead to increased continental cooling and aridification, which would then cause perturbations in terrestrial biota through reduced food availability. These deteriorating conditions, in turn, could lead to habitat fragmentation and extinction on the one hand, and to migration and lineage splitting on the other hand. The low proportions of humidity-indicating rodents and insectivores during Miocene obliquity nodes that are covered by rich and well-dated localities (16.1–15.8, 15.2–14.95, 13.85–13.6, 9.2–8.75, 8.15–7.7 Myr ago) confirm the presence of temporarily drier conditions (Supplementary Fig. 7). The lithological equivalents of these intervals are dominated by (or contain the transition to) red bed units, which represent the drier phases in the red bed—limestone alternations that are characteristic for the study area[20–22]. In contrast, Pliocene obliquity nodes correlate with limestone-rich intervals[23], and are not associated with distinct positive or negative peaks in the proportion of humidity-adapted small mammals (5.3–2.5 Myr ago; Supplementary Fig. 7). Unfortunately, there are few high-resolution, well-dated Miocene–Pliocene humidity proxy records straddling obliquity nodes with which to make a comparison. Pliocene pollen assemblages from northwestern Africa associated with oxygen isotope stages 130 and 134 (Mammoth-Gauss 2 event; Fig. 3g) at 3.3 Myr ago[24] point to drier conditions for this region during the associated obliquity node. High carbonate levels in the Mediterranean sea[25] during the Miocene-isotope-5 $\delta^{18}O$ event at 11.6–11.4 Myr ago[14] also seem to confirm the occurrence of drier regional conditions during Miocene nodes of obliquity.

The second dominant type of turnover occurs during eccentricity minima with a mean spacing of 2.37 Myr before 6 Myr ago, and also seems to be associated with climate-induced changes. Closer inspection of the four best-dated turnovers between 17 and 7 Myr ago (Fig. 3b) indicates that these tend to be concentrated at the fringes of these minima, where they correspond to strong 405-kyr eccentricity minima (Fig. 3d, e). A number of major $\delta^{18}O$ events are associated with this type of orbital configuration, for example, the Miocene-isotope-3a event at 14.2 Myr ago, peaks associated with the Miocene-isotope-7 event between 9.6–8.8 Myr ago, and two strong Tortonian-Messinian glaciations at 7.3–7.2 and 7.0–6.9 Myr ago (Fig. 3g; Supplementary Table 2). Also the events of Miocene-isotope-1a at 21.1 Myr ago, Miocene-isotope-1aa at 19.4 Myr ago, Sidufjall 4/6 at 4.85 Myr ago, and the glacial interval associated with isotope stages 98/100 at 2.4 Myr ago are associated with this configuration, indicating that low-amplitude eccentricity conditions favour global cooling and ice build-up even in the absence of low-amplitude obliquity changes. But in contrast to obliquity nodes, the proportions of humidity-adapted rodents and insectivores are high during eccentricity minima (Supplementary Figs 2, 3 and 7). The highest proportions occur at 16.7, 14.4–14.3, 12.1, 9.7–9.6 and 7.3 Myr ago (Supplementary Fig. 7), when 405-kyr minima are combined with high-amplitude obliquity. This observation is in accordance with our interpretation of more arid conditions during low-amplitude obliquity. Most of the wet-adapted small mammals that enter the record at these moments are immigrants with Central European source areas. Their southward expansions during periods of low eccentricity (mean spacing of 2.37 Myr) can be interpreted as a direct, regional response to changes in the Mediterranean precipitation regime[26,27].

The presence of major carbonate units indicative of lake expansion at stratigraphical positions corresponding to 2.37-Myr eccentricity minima[20–22] is consistent with the higher humidity levels at these intervals as inferred from the small mammals. Moreover, detailed cyclostratigraphical analysis shows the expected weakening in the expression of predominantly precession-controlled sedimentary cycles during 405-kyr eccentricity minima that coincide or closely coincide with the 2.37-Myr minima[13,22]. Recent climate modelling experiments show that western Mediterranean summers are warmer and drier during a circular Earth orbit (zero eccentricity and no precessional effects) than during a precession maximum (at maximum eccentricity), but cooler and more humid than during a precession minimum (at maximum eccentricity; E. Tuenter, personal communication and ref. 28). These results suggest that the prolonged absence of extreme summer conditions—characterized by strong evaporation—that normally occur during strong precession minima favours lake extension and leads to an increase of both wet-adapted small-mammal lineages and total diversity during minimum eccentricity (Fig. 1d). It can be argued that regional biogeographical and genetic processes raise turnover rates even further, because generalism and vagility (the ability to disperse), properties that would normally contribute to spatial and genetic remixing during successive climate swings, are temporarily less selected for during prolonged intervals without extreme climates. At the same time, specialization trends are expected to continue for a longer time during such intervals and to have a higher probability of leading to successful speciation[10,29]. These arguments are consistent with the observation that Pleistocene turnover rates are relatively low despite the occurrence of frequent and strong climatic events[9,10].

The apparent correlation between orbital configurations, climatic events and rodent turnover strongly suggests that the latter is controlled by astronomically forced climate change. Most intervals of no correlation either correspond to Miocene intervals during which amplitudes and durations of the orbital parameters do not reach specific threshold values (Fig. 3d; Supplementary Table 2), or to the Pliocene, for which additional relationships between long-term astronomical cycles and climate have been proposed, including a forcing of bipolar ice-sheet growth by maximum obliquity variation[12] (Fig. 3f, g).

The postulated astronomical hypothesis for species turnover provides a crucial missing piece in the puzzle of mammal species- and genus-level evolution, and provides a probable mechanism to explain third-tier processes. The new hypothesis is consistent with the Turnover Pulse hypothesis[3] in the sense that lineage events tend to cluster and that the clusters correlate to abiotic events. In addition, the astronomical hypothesis for turnover offers a plausible explanation for the characteristic duration of ~2.5 Myr of the mean species lifespan in mammals, and may explain similar durations in other biological groups as well.

METHODS

Age uncertainties surrounding poorly constrained localities and first- and last-appearance datums were addressed by generating 1,000 equally probable, equally spaced (0.1 Myr) time series ('age models') for origination, extinction and turnover (sum of origination and extinction) for the entire study interval. The final target series used consisted of the means of all 1,000 series. The 1,000 time series were produced by combining 50 locality age models with 20 sets of random draws from the uncertainty intervals preceding first appearances or succeeding last appearances. These intervals were calculated on the basis of sample size by calculating the probability of finding a taxon in preceding (or succeeding) localities given the proportion in the locality where it was first (or last) recorded, and using a cut-off value of 80% (ref. 7). The same procedures were applied to range gaps. These were defined as true gaps if the midpoints of the uncertainty intervals differed by 1.0 Myr or more, in which case the lineage was split for the subsequent analyses. In the cases of gaps less than 1.0 Myr, the taxon was considered to have remained present (range-through approach; see Supplementary Notes for more details).

Clustering of events was tested by running a separate bootstrap analysis for each of the 1,000 sets of origination, extinction and turnover. The analyses involved the comparison of observed numbers of events per moving 0.3-Myr interval (the chosen bootstrap test statistic) with the corresponding numbers of events from 1,000 rounds of randomly reshuffling 0.1-Myr level first- and last-appearance ages of all lineages across the presence intervals of their families. The final significance levels were calculated as the average levels over the 1,000 time series. Each individual level was calculated as the midpoint of that part of the cumulative relative frequency distribution (of the number of events resulting from the 1,000 rounds of reshuffling) that corresponded to the observed number of events. Significant intervals are included in Supplementary Table 2.

Received 16 January; accepted 11 August 2006.

1. Alroy, J. New methods for quantifying macroevolutionary patterns and processes. *Paleobiology* **26**, 707–733 (2000).
2. Vrba, E. S. & DeGusta, D. Do species populations really start small? New perspectives from the Late Neogene fossil record of African mammals. *Phil Trans. R Soc Lond. B* **359**, 285–293 (2004).
3. Vrba, E. S. in *Paleoclimate and Evolution, with Emphasis on Human Origins* (eds Vrba, E. S., Denton, G. H., Partridge, T. C. & Burckle, L. H.) 385–424 (Yale, New Haven, 1995).
4. Barnosky, A. D. Distinguishing the effects of the Red Queen and Court Jester on Miocene mammal evolution in the Northern Rocky Mountains. *J. Vertebr. Paleontol.* **21**, 172–185 (2001).
5. Prothero, D. R. & Heaton, T. H. Faunal stability during the Early Oligocene climatic crash. *Palaeogeogr. Palaeoclimatol. Palaeoecol.* **127**, 257–283 (1996).
6. Alroy, J., Koch, P. L. & Zachos, J. C. in *Deep Time: Paleobiology's Perspective* (eds Erwin, D. H. & Wing, S. L.) 259–288 (Paleontological Society, Lawrence, 2000).
7. Barry, J. *et al.* Faunal and environmental change in the Late Miocene Siwaliks of Northern Pakistan. *Paleobiol. Memoirs* **3**; suppl. to *Paleobiology* **28**, 1–71 (2002).
8. Laskar, J. *et al.* A long term numerical solution for the insolation quantities of the Earth. *Astron. Astrophys.* **428**, 261–285 (2004).
9. Bennett, K. D. *Evolution and Ecology: the Pace of Life* (Cambridge Univ. Press, 1997).
10. Dynesius, M. & Jansson, R. Evolutionary consequences of changes in species' geographical distributions driven by Milankovitch climate oscillations. *Proc Natl Acad. Sci. USA* **97**, 9115–9120 (2000).
11. Lourens, L. J., Hilgen, F. J., Laskar, J., Shackleton, N. J. & Wilson, D. in *A Geological Time Scale 2004* (eds Gradstein, F. M., Ogg, J. G. & Smith, A. G.) 409–440 (Cambridge Univ. Press, 2004).
12. Lourens, L. J. & Hilgen, F. J. Long-periodic variations in the Earth's obliquity and their relation to third-order eustatic cycles and late Neogene climate change. *Quat. Int.* **40**, 43–52 (1997).
13. Abdul Aziz, H., Krijgsman, W., Hilgen, F. J., Wilson, D. S. & Calvo, J. P. An astronomical polarity timescale for the late middle Miocene based on cyclic continental sequences. *J. Geophys. Res.* **108** (B3), 2159–2175 (2003).
14. Turco, E., Hilgen, F. J., Lourens, L. J., Shackleton, N. J. & Zachariasse, W. J. Punctuated evolution of global climate cooling during the late Middle to early Late Miocene: high-resolution planktonic foraminiferal and oxygen isotope records from the Mediterranean. *Paleoceanography* **16**, 405–423 (2001).
15. Zachos, J., Shackleton, N. J., Revenaugh, J. S., Pälike, H. & Flower, B. P. Climate response to orbital forcing across the Oligocene–Miocene boundary. *Science* **292**, 274–278 (2001).
16. Wade, B. S. & Pälike, H. Oligocene climate dynamics. *Paleoceanography* **19**, doi:10.1029/2004PA001042 (2004).
17. Westerhold, T., Bickert, U. & Röhl, U. Middle to late Miocene oxygen isotope stratigraphy of ODP site 1085 (SE Atlantic): new constrains on Miocene climate variability and sea-level fluctuations. *Palaeogeogr. Palaeoclimatol Palaeoecol.* **217**, 205–222 (2005).
18. Abels, H. A. *et al.* Long-period orbital control on middle Miocene global cooling: integrated stratigraphy and astronomical tuning of the Blue Clay Formation on Malta. *Paleoceanography* **20**, doi:10.1029/2004PA001129 (2005).
19. Zachos, J., Pagani, M., Sloan, L., Thomas, E. & Billups, K. Trends, rhythms, and aberrations in global climate 65 Ma to present. *Science* **292**, 686–693 (2001).
20. Daams, R. *et al.* Stratigraphy and sedimentology of the Aragonian (early to middle Miocene) in its type area (north-central Spain). *Newslett. Stratigr.* **37**, 103–139 (1999).
21. Alonso Zarza, A. M. & Calvo, J. P. Palustrine sedimentation in an episodically subsiding basin: the Miocene of the northern Teruel Graben. *Palaeogeogr. Palaeoclimatol. Palaeoecol.* **160**, 1–21 (2000).
22. Abdul Aziz, H., van Dam, J. A., Hilgen, F. J. & Krijgsman, W. Astronomical forcing in Upper Miocene continental sequences: implications for the Geomagnetic Polarity Time Scale. *Earth Planet. Sci. Lett.* **222**, 243–258 (2004).
23. Mein, P., Moissenet, E. & Adrover, R. Biostratigraphie du Néogène supérieur de Teruel. *Paleont. Evol.* **23**, 121–139 (1990).
24. Leroy, S. & Dupont, L. Development of vegetation and continental aridity in northwestern Africa during the Late Pliocene: the pollen record of ODP Site 658. *Palaeogeogr. Palaeoclimatol. Palaeoecol.* **109**, 295–316 (1994).
25. Hilgen, F. J., Abdul Aziz, H., Krijgsman, W., Raffi, I. & Turco, E. Integrated stratigraphy and astronomical tuning of the Serravallian and lower Tortonian at Monte dei Corvi (Middle-Upper Miocene, northern Italy). *Palaeogeogr. Palaeoclimatol. Palaeoecol.* **199**, 229–264 (2003).
26. van Dam, J. A. & Weltje, G. J. Reconstruction of the late Miocene climate of Spain using rodent paleocommunity successions: an application of end-member modelling. *Palaeogeogr. Palaeoclimatol. Palaeoecol.* **151**, 267–305 (1999).
27. van Dam, J. A. Anourosoricini (Soricidae, Mammalia) from the Mediterranean Region: a pre-Quaternary example of recurrent climate-controlled North-South range shifting. *J. Paleontol.* **78**, 741–764 (2004).
28. Tuenter, E. *Modeling Orbital Induced Variations in Circum-Mediterranean Climate*. PhD thesis, Utrecht Univ. (2004).
29. Sheldon, P. R. Plus ça change—a model for stasis and evolution in different environments. *Palaeogeogr. Palaeoclimatol. Palaeoecol.* **127**, 209–227 (1996).
30. Heslop, D. & Dekkers, M. J. Spectral analysis of unevenly spaced climatic time series using CLEAN; signal recovery and derivation of significance levels using a Monte Carlo simulation. *Phys. Earth Planet. Inter.* **130**, 103–116 (2002).